Title: Poster Previews

Speakers:

Collection: Quantum Matter Workshop

Date: November 14, 2022 - 3:15 PM

URL: https://pirsa.org/22110067

Abstract: 3:15PM Arnab Adhikary
3:18PM Anjishnu Bose
3:21PM Matthew Duschenes
3:24PM SangEun Han & Daniel Schultz
3:27PM Andrew Hardy
3:30PM Daniel Huerga
3:33PM Vedangi Pathak
3:36PM Shengqi Sang
3:39PM Joseph Tindall
3:42PM Tarun Tummuru
3:45PM Ryohei Weil
3:48PM Rui Wen
3:51PM Ye Weicheng
3:54PM Emily Zhang

Chiral Broken Symmetry Descendants of the Kagomé Lattice Chiral Spin Liquid

Anjishnu Bose[1], Arijit Haldar[1], Erik S. Sørensen[2], Arun Paramekanti[1]
[1] University of Toronto, [2] McMaster University

Abstract

- Using **Spin-wave theory, ED, MFT, and VMC**, we uncover two chiral magnetic orders – *XYZ and Octahedral order* – near the gapped CSL on the kagomé lattice, which are accessed by tuning a small Heisenberg interaction across the bow-ties.
- Our proposed global phase diagram, as we vary spin S, hints at the possibility of unusual QSLs in the chiral model for higher spin, including spin-1 magnets.
- Our work unveils distinct non-coplanar orders on the kagomé lattice, and points to a **universal connection between many-body topological order in the gapped CSL and real-space topology**, consistent with previous ED and DMRG results.

References

[1] Anjishnu Bose, Arijit Haldar, Erik S. Sørensen, and Arun Paramekanti, "Chiral Broken Symmetry Descendants of the Kagomé Lattice Chiral Spin Liquid," April 2022, 10.48550/ARXIV.2204.10329

Partonic trial wave-functions

Express spins using **Abrikosov fermions**, with the constraint of one fermion/site as

$$\boldsymbol{S}_i = \frac{1}{2} f_i^{\alpha\dagger} \boldsymbol{\sigma}_{\alpha\beta} f_i^{\beta}, \quad f_i^{\alpha\dagger} f_i^{\alpha} = 1. \tag{2}$$

Use a trial fermion Hamiltonian consisting of complex hoppings with fluxes, and Weiss fields at every site which are indicative of magnetic ordering when it sets in.

$$\mathcal{H}_{trial} = -\sum_{i,j} t_{ij} \sum_{\alpha} \left(e^{-\iota\phi_{ij}} f_i^{\alpha\dagger} f_j^{\alpha} + h.c. \right) - \mathcal{B} \sum_i f_i^{\alpha\dagger} \left(\hat{\boldsymbol{b}}_i . \boldsymbol{\sigma} \right)_{\alpha\beta} f_i^{\beta}. \tag{3}$$

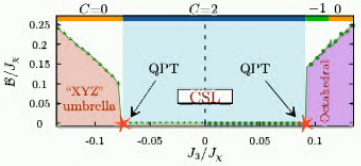

Figure 2: Mean-field theory : phase diagram of the parton theory for a 12×12 lattice, as we vary J_3/J_χ showing transition to the *Octahedral* state for $J_3 > J_3^{Oct} > 0$, and the *XYZ-umbrella* state for $J_3 < J_3^{XYZ} < 0$. Top line depicts the corresponding total Chern number of the half-filled parton bands in various phases.

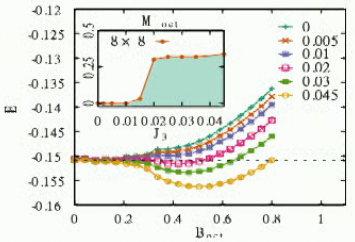

Figure 3: Gutzwiller wavefunction study. Variational energy versus $\mathcal{B}_{wf}$ for an 8×8 lattice for different J_3, showing a stable CSL state for $J_3 = 0$ and an instability to Octahedral order for $J_3 \gtrsim 0.02$. Inset shows the order parameter $\mathcal{M}_{oct}$.

Model

Our spin model on the kagomé lattice hosts a **chiral interaction** between three spins on every triangle, and a **Heisenberg interaction** between two spins across every bow-tie.

$$H_S = -J_\chi \sum_{\triangle,\triangledown} \boldsymbol{S}_i \cdot \boldsymbol{S}_j \times \boldsymbol{S}_k + J_3 \sum \boldsymbol{S}_i \cdot \boldsymbol{S}_j. \tag{1}$$

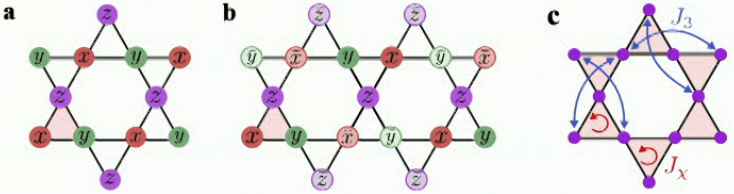

Figure 1: **a** The XYZ umbrella magnetic ordering. **b** The Octahedral magnetic ordering. **c** The chiral three-spin interactions and bow-tie two-spin couplings in H_S.

Spin-wave theory

We use the **Holstein-Primakoff transformation** on locally rotated spins, $\tilde{\boldsymbol{S}}_{n,j} = R_j \cdot \boldsymbol{S}_{n,j}$, and calculate the average quantum correction to $\langle \tilde{S}^z_{n,j} \rangle$ upto $O(1/S)$.

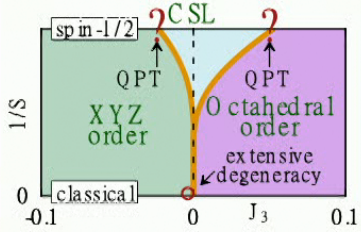

Figure 4: Proposed phase diagram of H_S as we tune J_3 and the strength of quantum fluctuations via linear spin-wave theory.

Exact diagonalization

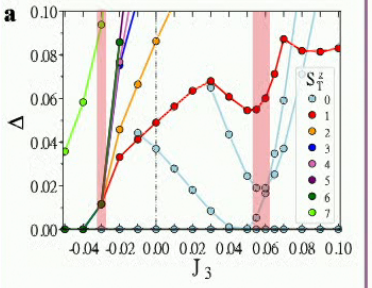

Figure 5: Energy gaps to the lowest lying states in each S^z_T sector versus J_3.

NSERC CRSNG

UNIVERSITY OF TORONTO

Microscopic theory of multi-stage Fermi surface reconstruction

SangEun Han, Daniel J. Schultz, Yong Baek Kim

University of Toronto

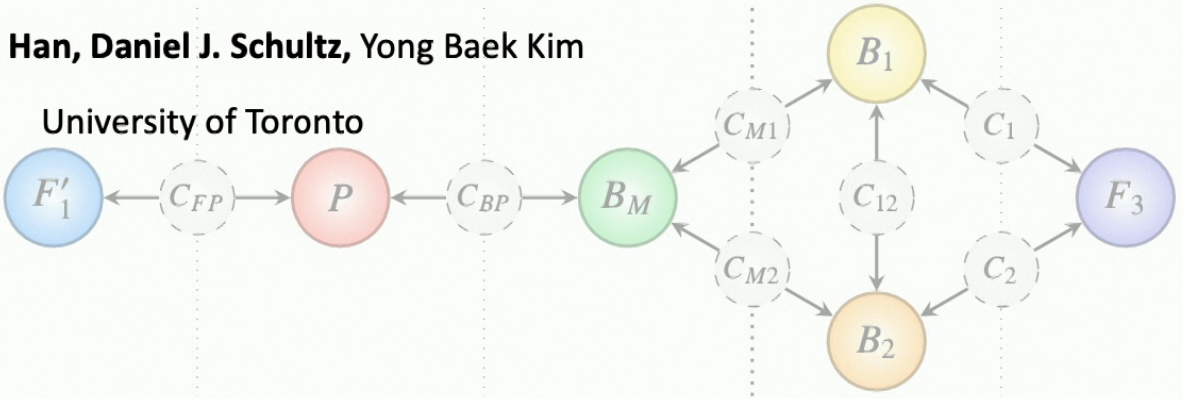

Crystal field splitting

Ce^{+3}

$4f^1$

$j=5/2$

Crystal Electric Field Splitting

Point group symmetry (8c)

T_d

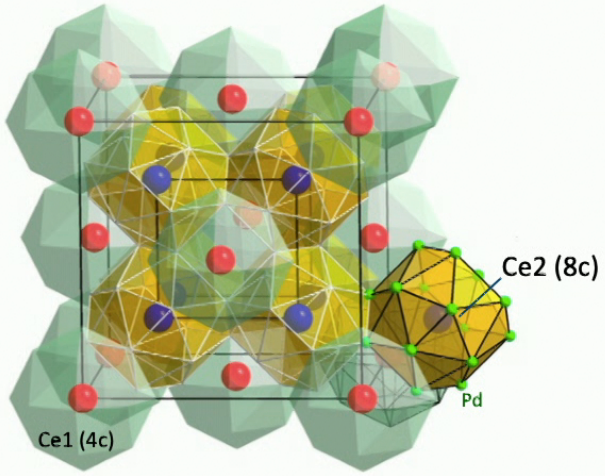

$Ce_3Pd_{20}Si_6$

(8c, T_d)

Γ_7 44K

Γ_8 0

S. Paschen, et al (2008)

Crystal field splitting

S. Paschen, et al (2008)

Ce^{+3}

$4f^1$

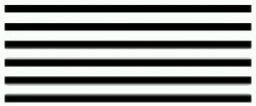

j=5/2

Crystal Electric Field Splitting

Point group symmetry (8c)

T_d

$Ce_3Pd_{20}Si_6$

(8c, T_d)

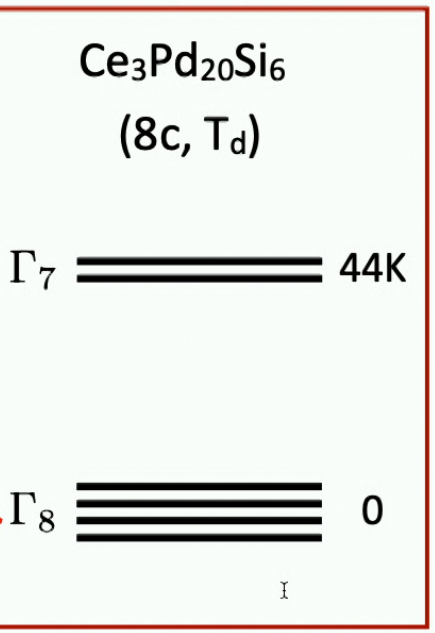

Γ_8 Quartet

$$\Gamma_8^{(1)} = \sqrt{\frac{5}{6}}|+\frac{5}{2}\rangle + \sqrt{\frac{1}{6}}|-\frac{3}{2}\rangle, \quad \Gamma_8^{(3)} = |+\frac{1}{2}\rangle,$$

$$\Gamma_8^{(2)} = \sqrt{\frac{5}{6}}|-\frac{5}{2}\rangle + \sqrt{\frac{1}{6}}|+\frac{3}{2}\rangle, \quad \Gamma_8^{(4)} = |-\frac{1}{2}\rangle.$$

Moments	Irrep.	
Dipolar	T_1	: 3
Quadrupolar	E, T_2	: 5
Octupolar	A_2, T_1, T_2	: 7

→ 15 multipolar moments

Two-stage Fermi-surface reconstruction QPT

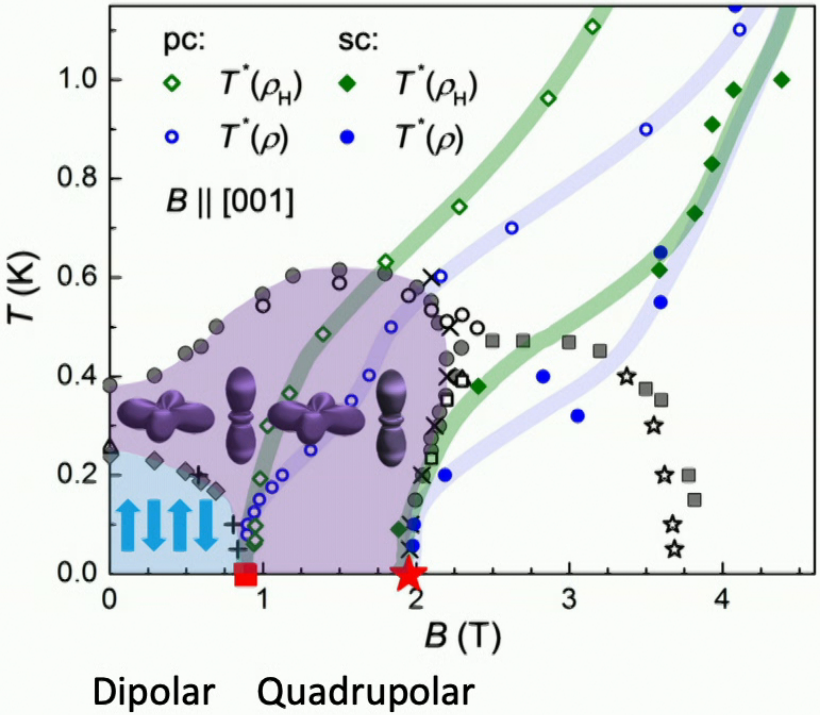

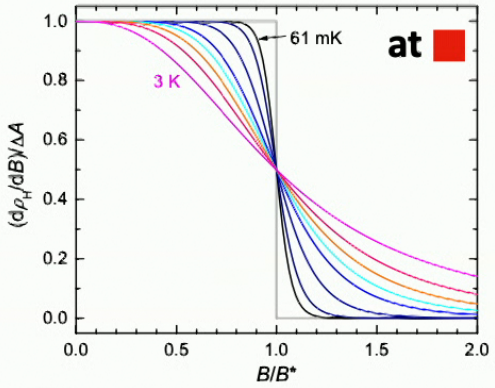

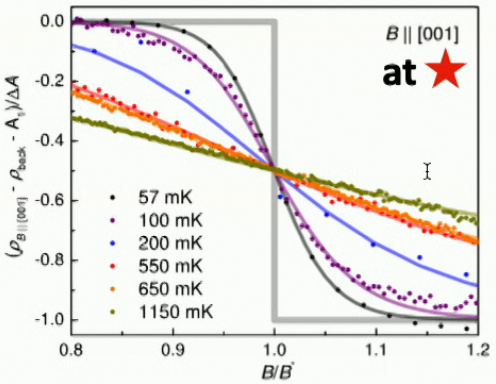

: Sharp drop
in Hall resistivity $\rho_H = \frac{h}{e^2 n}$

→ Enlarging Fermi surface

→ Two-stage Fermi-surface reconstruction QPT with multipolar ordering

Multipolar Kondo lattice problem

NEMATIC ORDER FROM A MULTIORBITAL STRANGE METAL

ANDREW HARDY, ARIJIT HALDAR, & ARUN PARAMEKANTI

ABSTRACT

- We study a two-orbital lattice extension of the Sachdev-Ye-Kitaev model in the large-N limit.
- The phase diagram features multicritical nematic ordering.
- We explore the thermodynamic, spectral, and transport properties, including the elastoresitivity.
- Our work offers a useful perspective on nematic phases and transport in correlated multiorbital systems.

THE MODEL

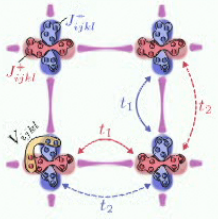

Each square lattice site ($\mathbf{r}$) is occupied by two SYK orbitals (red (+) and blue (−) circles). Each orbital has an SYK-type self-interaction ($J^{\pm}_{ijkl}(\mathbf{r})$) and an inter-orbital SYK-type interaction ($V_{ijkl}(\mathbf{r})$). Orbitals on neighboring lattice sites are connected via anisotropic hoppings with an 'easy' axis ($t_1 = t + \delta t$) and a 'hard' axis ($t_2 = t - \delta t$).

$$H_{\text{kin}} = \sum_{\mathbf{k},s,i} \varepsilon_s(\mathbf{k}) c^\dagger_{\mathbf{k},s,i} c_{\mathbf{k},s,i}$$

PHASE DIAGRAM

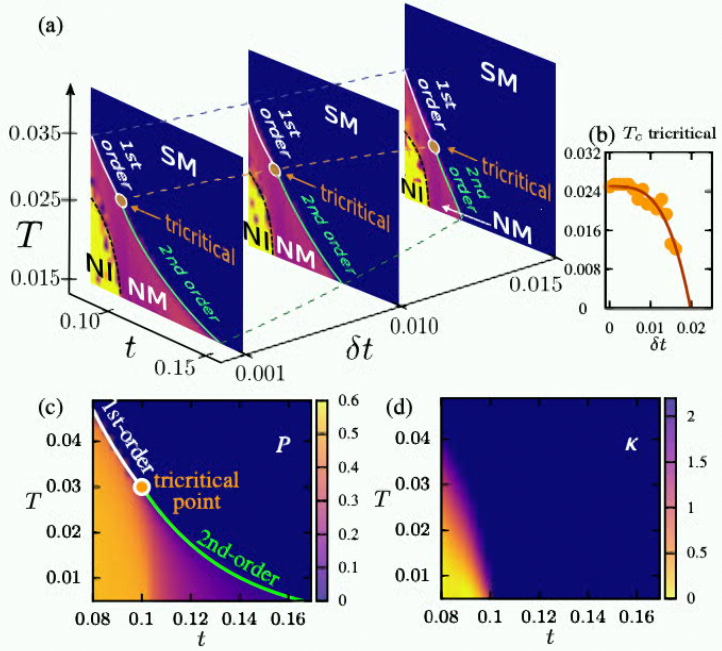

(a) Phase diagram in terms of temperature (T), hopping (t), and hopping anisotropy δt, showing an isotropic strange metal (SM), a nematic metal (NM), and a nematic insulator (NI). The isotropic and nematic phases are separated by first-order or continuous thermal transitions which meet at a tricritical point (filled circle). The NM and NI regimes are separated by a crossover at nonzero T. (b) Temperature at the tricritical point versus δt showing that it could be potentially further tuned to reach a quantum tricritical point with different strain. (c) Polarization ($P = \langle n_+ \rangle - \langle n_- \rangle$), or orbital density imbalance. (d) Compressibility ($\kappa = \langle n \rangle^{-2} \partial \langle n \rangle / \partial \mu$), distinguishing metallic from insulating phases.

DISCUSSION

TRANSPORT

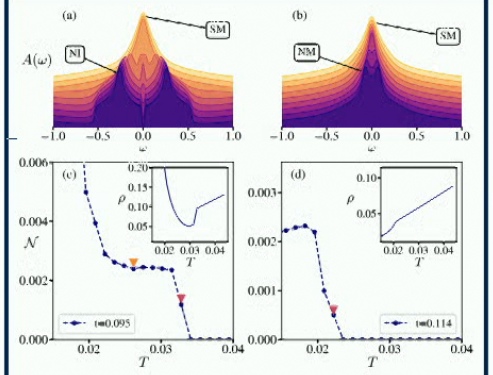

Evolution of spectral function $A(\omega)$ with temperature T as a function of frequency ω. Resistive nematicity $\mathcal{N} = (\rho_{xx} - \rho_{yy})/(\rho_{xx} + \rho_{yy})$ which is zero in the SM phase, increases and saturates in the NM, and further rapidly increases at low T in the NI regime. Inset shows the average resistivity $\rho(T) = (\rho_{xx} + \rho_{yy})/2$.

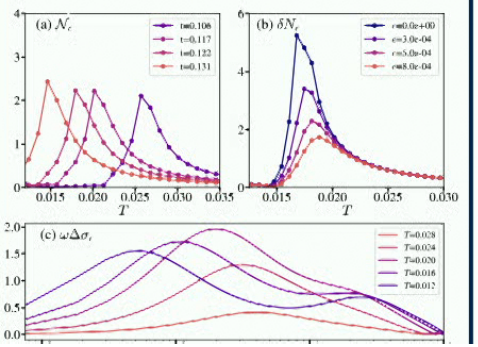

Revealing the nature of magnetic interactions by inelastic neutron scattering measurements on the honeycomb magnet $BaCo_2(AsO_4)_2$

A comprehensive inelastic neutron scattering study on the Kitaev candidate BCAO.
We examine two leading theoretical models: the Kitaev-type JKΓΓ′ model and the XXZ-J1-J3 model.

Felix Desrochers, Emily Z. Zhang,
Thomas Halloran, Collin Broholm, Yong Baek Kim

UNIVERSITY OF TORONTO

Variational Quantum Simulation of VBS

H

$S = 1/2$

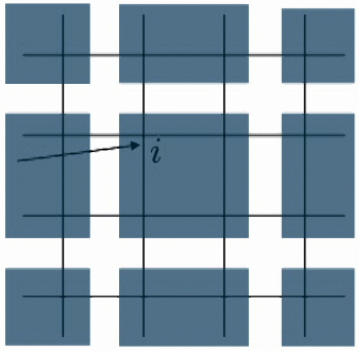

cluster-Gutzwiller ansatz

$$|\Psi(\boldsymbol{\theta})\rangle = \prod_{\square} |\psi(\boldsymbol{\theta})\rangle$$

equivalent to

$H_{\square} + H_{\mathrm{mf}}$

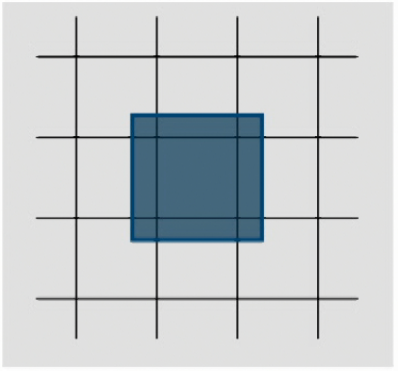

exact limit

$N \to \infty$

=> Scaling

Classically $N_{\max} \simeq 30$

Variational Quantum Simulation of VBS

H

$S = 1/2$

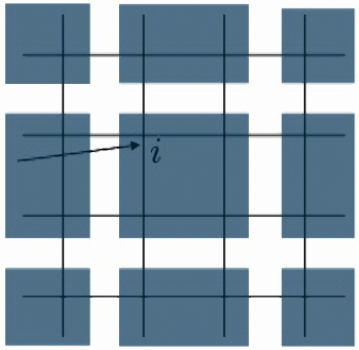

cluster-Gutzwiller ansatz

$$|\Psi(\boldsymbol{\theta})\rangle = \prod_{\square} |\psi(\boldsymbol{\theta})\rangle$$

equivalent to

$H_{\square} + H_{\mathrm{mf}}$

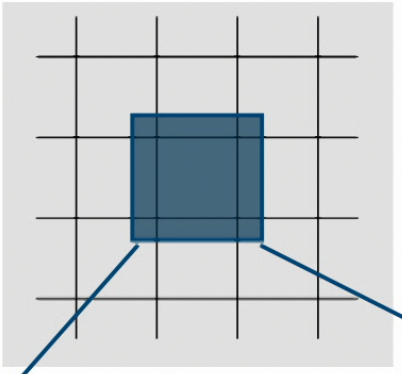

exact limit

$N \to \infty$

=> Scaling

Parameterized Quantum Circuit

$$|\psi(\boldsymbol{\theta})\rangle = \mathcal{U}(\boldsymbol{\theta}) |\psi_0\rangle$$

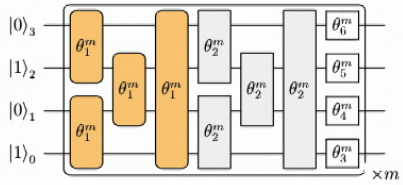

Classical optimizer

$$\min_{\boldsymbol{\theta}} \langle\Psi(\boldsymbol{\theta})| H |\Psi(\boldsymbol{\theta})\rangle \geq E^{\mathrm{exact}}$$

Variational Quantum Simulation of VBS

Benchmark: J1-J2 Heisenberg AFM

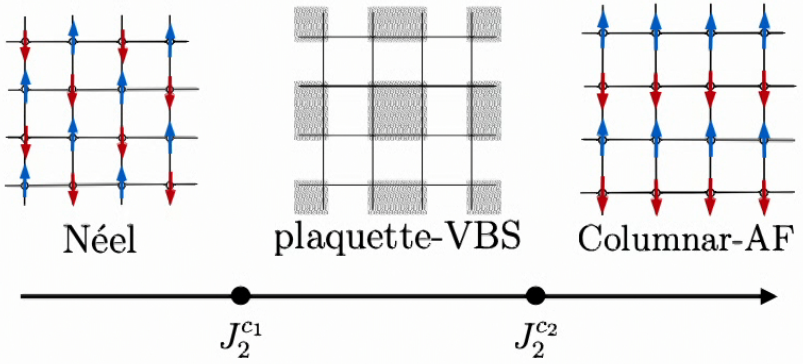

$H_\square + H_{\text{mf}}$

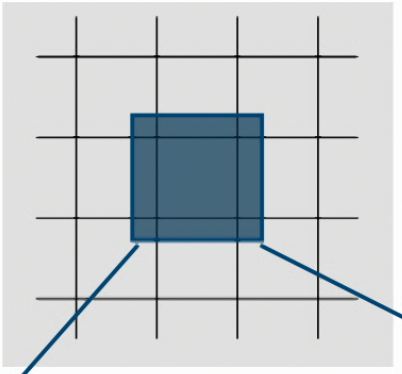

exact limit

$N \to \infty$

=> Scaling

Classical optimizer

$$\min_{\boldsymbol{\theta}} \langle \Psi(\boldsymbol{\theta}) | H | \Psi(\boldsymbol{\theta}) \rangle \geq E^{\text{exact}}$$

Parameterized Quantum Circuit

$$|\psi(\boldsymbol{\theta})\rangle = \mathcal{U}(\boldsymbol{\theta}) |\psi_0\rangle$$

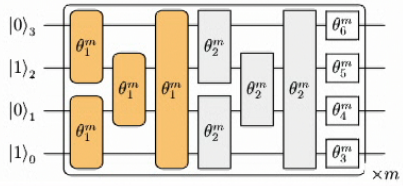

Variational Quantum Simulation of VBS

Benchmark: J1-J2 Heisenberg AFM

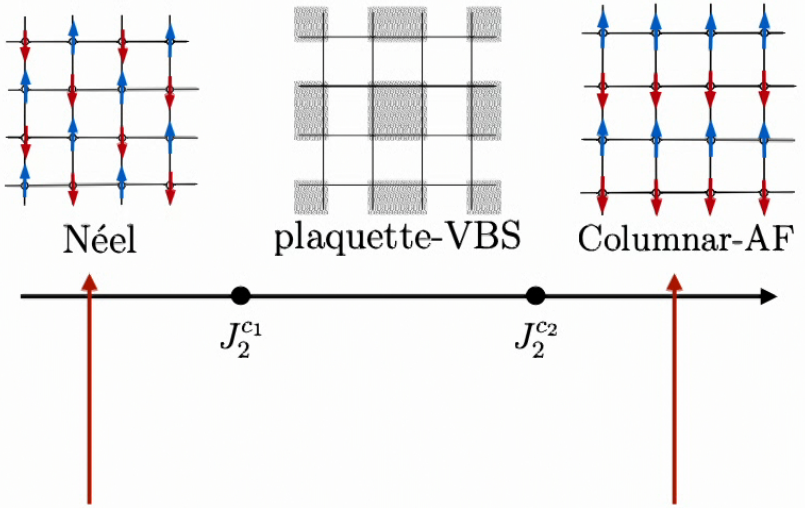

convergence pushed by LRO

$H_\square + H_{\text{mf}}$

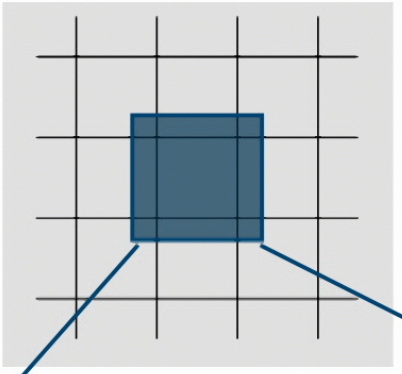

exact limit

$N \to \infty$

=> Scaling

Parameterized Quantum Circuit

$$|\psi(\boldsymbol{\theta})\rangle = \mathcal{U}(\boldsymbol{\theta})\,|\psi_0\rangle$$

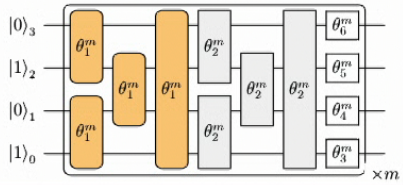

Counter intuitive yet efficient regimes of computation in (finite) SPT ordered chains

- Central question: Given a short range entangled symmetric state (supported on a 1D chain), how can we best use it for computation using local measurements?
- Measurement based quantum computation: proper initial state (resource) + local measurements simulates unitary evolution.

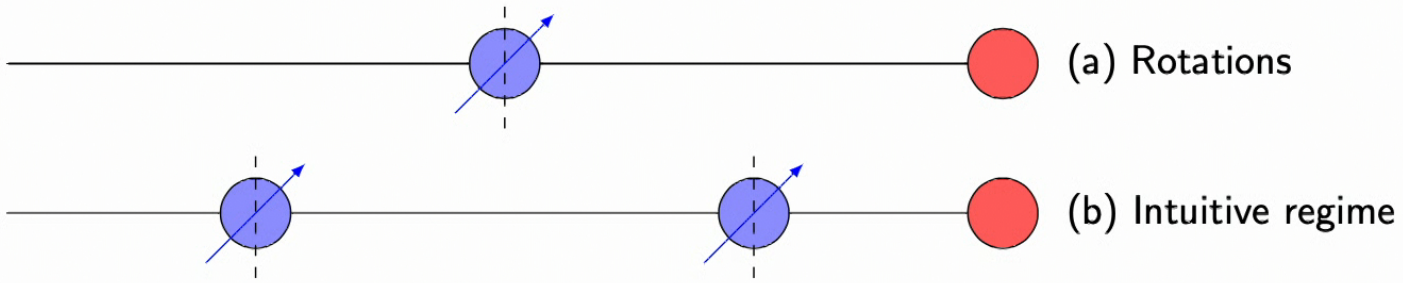

Counter intuitive yet efficient regimes of computation in (finite) SPT ordered chains

- Central question: Given a short range entangled symmetric state (supported on a 1D chain), how can we best use it for computation using local measurements?
- Measurement based quantum computation: proper initial state (resource) + local measurements simulates unitary evolution.

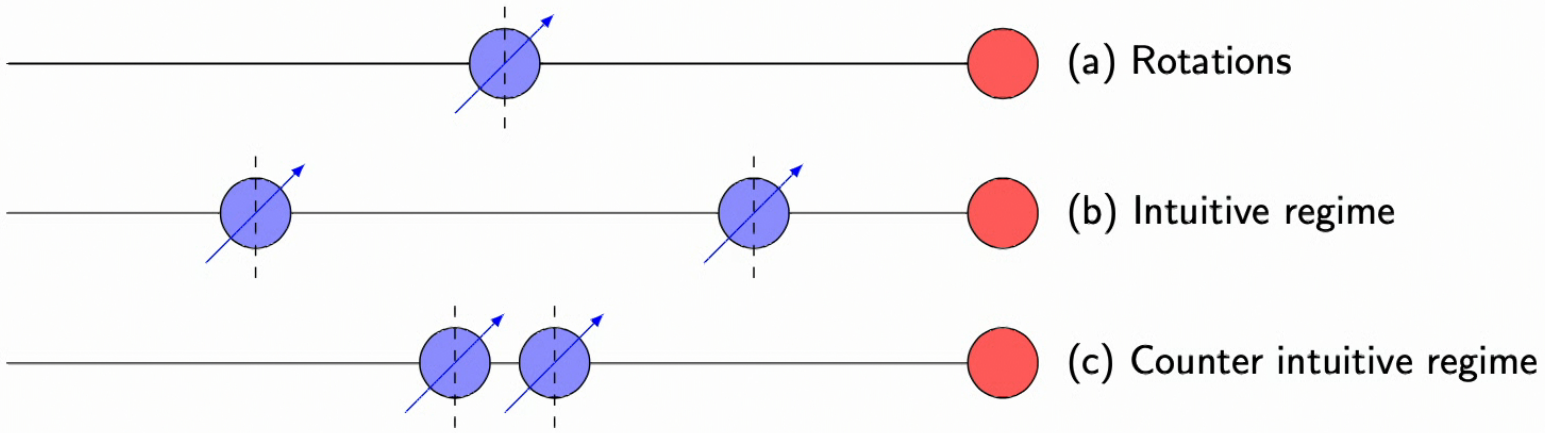

Majorana modes in a hybrid superconducting and magnetic vortex

1. What is a hybrid vortex?
2. Can it host Majorana modes?
3. What is interesting about the topology of the system?

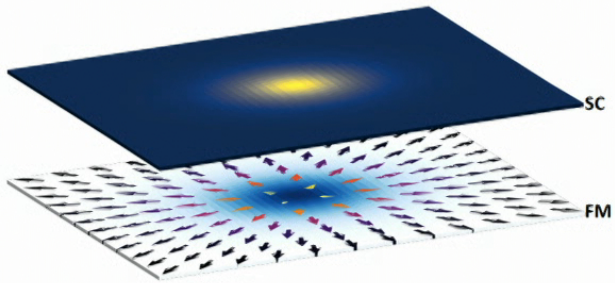

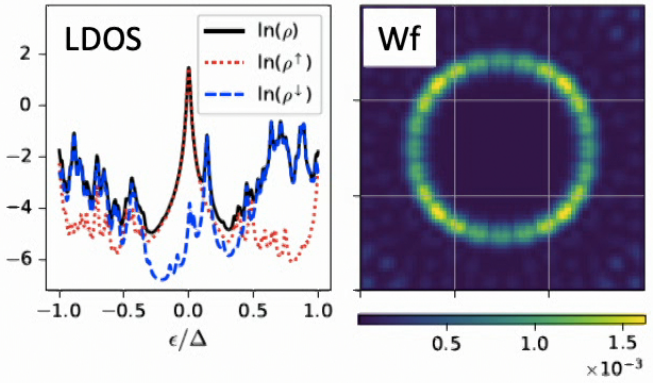

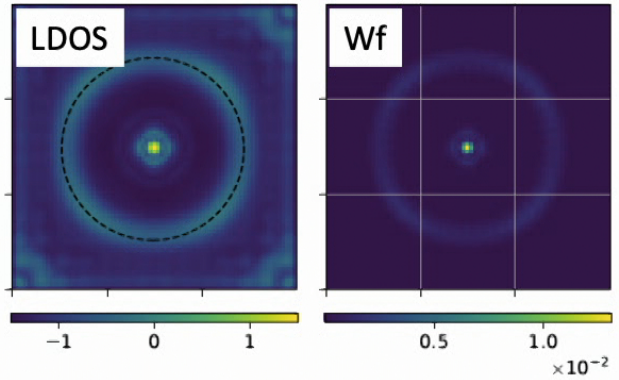

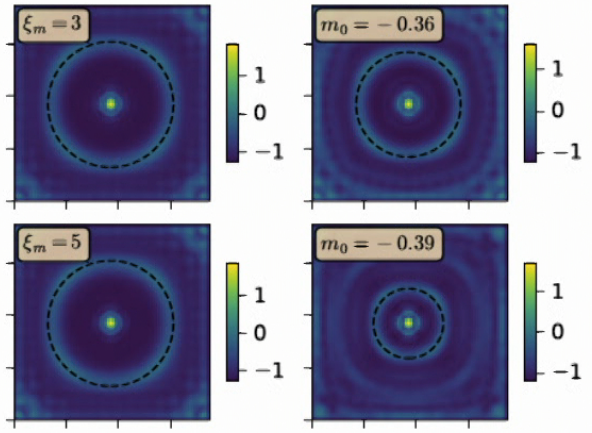

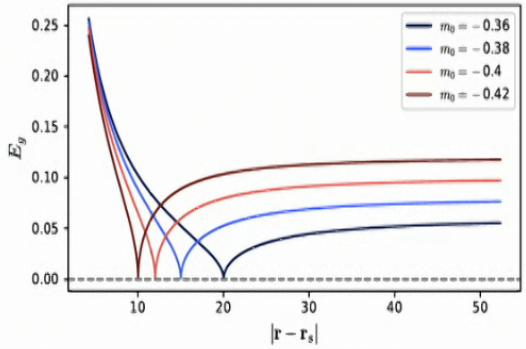

Investigating computational phases of matter on NISQ devices

SPT (Cluster) phase

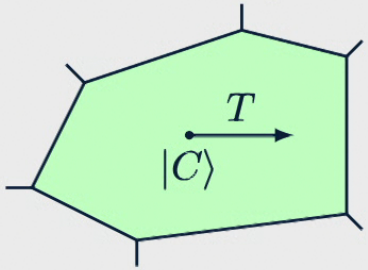

$=$

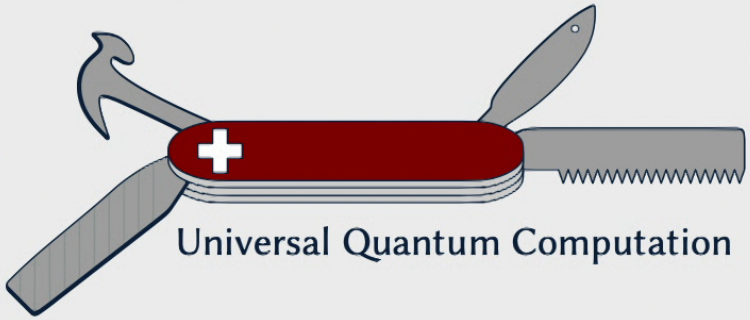

Universal Quantum Computation

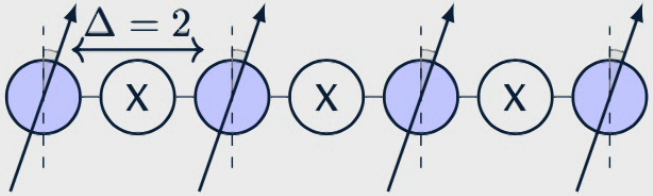

Efficient Techniques

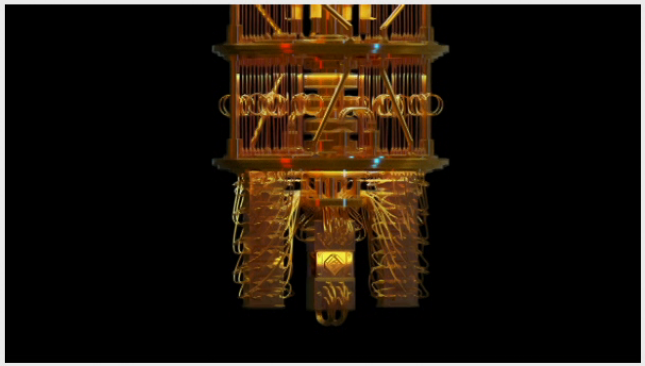

On NISQ devices

Introduction

1. Traditional topological phases of matter are associated with gapped systems where the gap can protect the robustness of topological properties.
2. Recent studies have shown rich topological properties could arise in gapless systems with edge modes that can not exsist in gapped systems.(igSPT)
3. In igSPT models studied before, there is a gapless sector of the system that possess an anomalous symmetry action U^A_{IR} which protects gaplessness.
4. The anomaly is lifted by UV DOF so that we can expose the edge of the system and study edge modes.

igSPT in a 1-d spin chain

The model:

$$H = H_0 + H_\Delta$$

$$H_0 = -J\sum_i \left(\tau^x_{i-1}\tau^x_i + \tau^y_{i-1}\tau^y_i\right)\sigma^x_i \quad H_\Delta = -\Delta\sum_i \sigma^z_i\ \tau^z_i\ \sigma^z_{i+1}$$

1. Low energy sector described by a gapless Luttinger liquid.
2. Non-anomalous exact $\mathbb{Z}_4$ symmetry.
3. Emergent $\mathbb{Z}_2$ anomaly in the IR, which protects gaplessness.
4. 2-fold GSD due to topological edge modes.

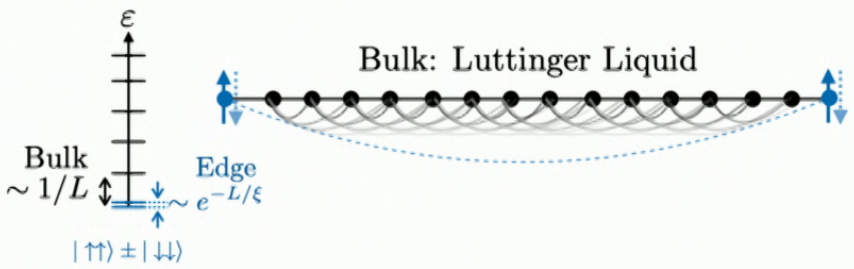

igSPT, Systematical study

Start with an in-cohomogy anomaly characterized by a cocycle $\omega_{D+2} \in H^{D+2}(G, U(1))$, together with a group extension $1 \to \mathcal{N} \to \Gamma \to G \to 1$, we can fractorize the anomaly as $\omega_{D+2} = b_D \cup e_2$ and construct a lattice model in D dimension with

1. exact anomalous-free Γ-symmetry,
2. IR gapless sector with emergent G-anomaly,
3. UV symmetry $U_n, n \in \mathcal{N}$ acts on the edge of the system and pumps a $(D-1)$d SPT with anomaly $b_D \cup n$.
4. Therefore the edge must sits at the critical points of SPT transitions.

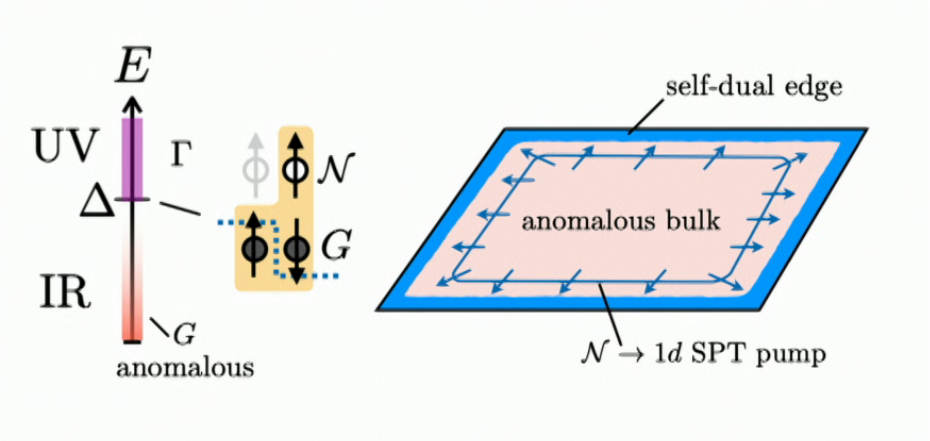

Twisted multilayer cuprates

Chiral twist

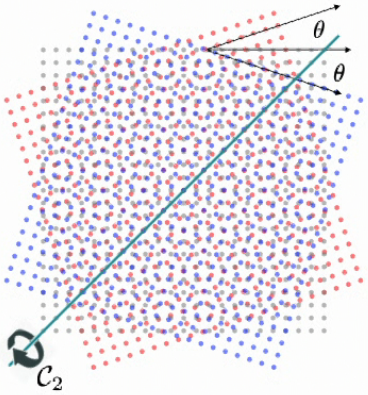

Alternating twist

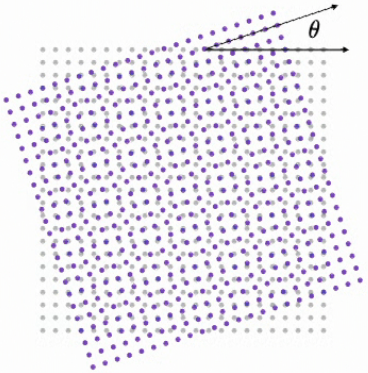

Twisted multilayer cuprates

Chiral twist

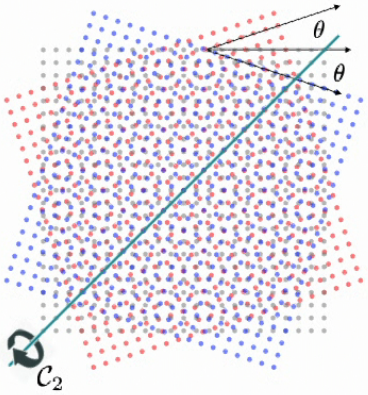

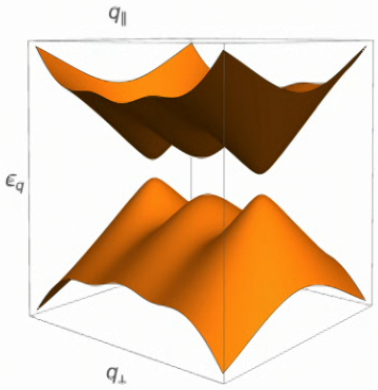

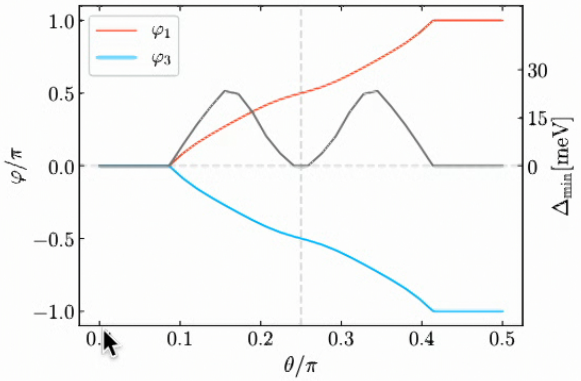

Alternating twist

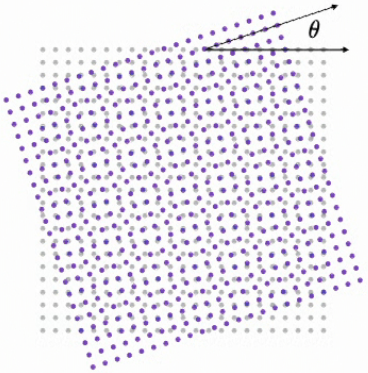

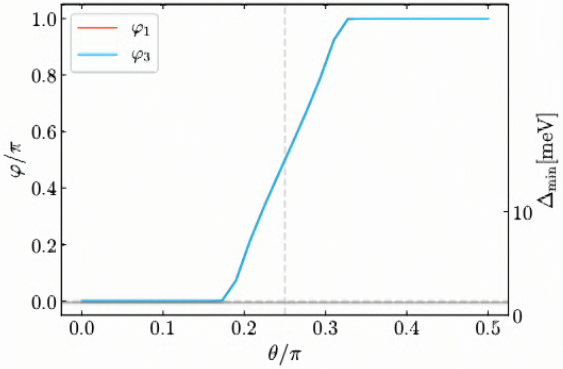

Twisted multilayer cuprates

Chiral twist

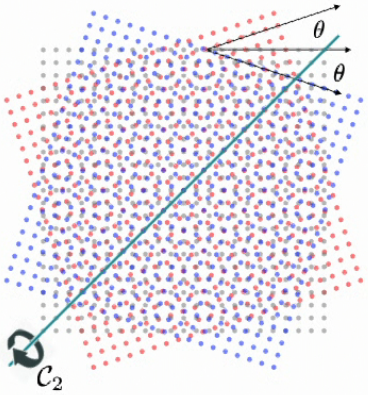

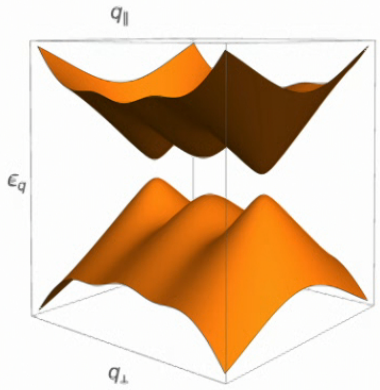

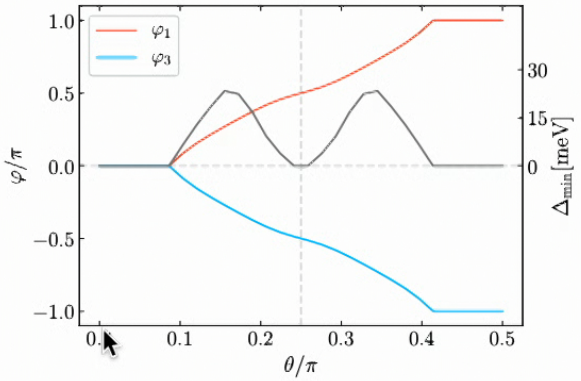

Alternating twist

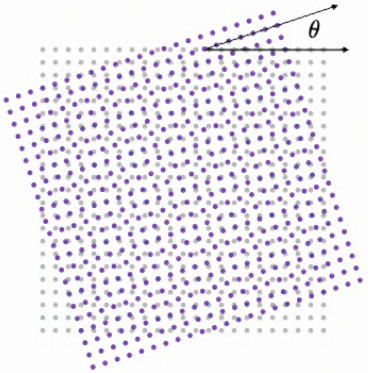

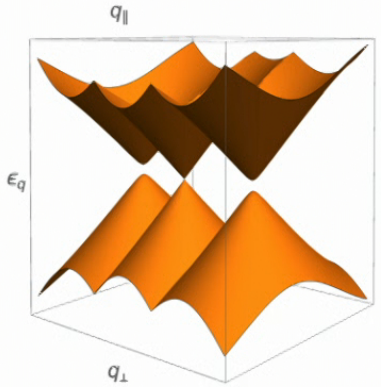

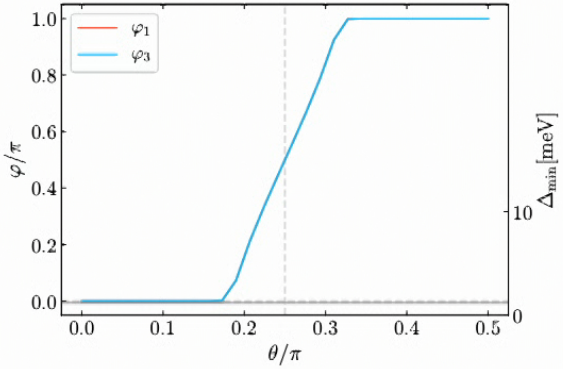

Floquet Codes with a Twist

Arpit Dua[1,4], Tyler Ellison[3], Joseph Sullivan[4,5], Nathanan Tantivasadakarn[4,6]

1. Department of Physics, California Institute of Technology, Pasadena, CA 91125, USA
3. Institute for Quantum Information and Matter, California Institute of Technology, Pasadena, California 91125, USA
5. Department of Physics, Yale University, New Haven, CT 06511, USA
4. Stewart Blusson Quantum Matter Institute, University of British Columbia, Vancouver, BC, Canada V6T 1Z1
6. Walter Burke Institute for Theoretical Physics, California Institute of Technology, Pasadena, CA 91125, USA
6. Department of Physics, Harvard University, Cambridge, MA 02138, USA

Background on Floquet codes

- Error correcting code inspired by the Kitaev honeycomb model
- Measurement schedule has three steps, involving measurement of two-body operators. After each round, half the qubits form a toric code eigenstate.
- Toric code is "moved around" in Hilbert space but logical information is preserved: dynamical logical qubit.
- Schedule constantly updates stabilizer eigenvalues allowing for error correction

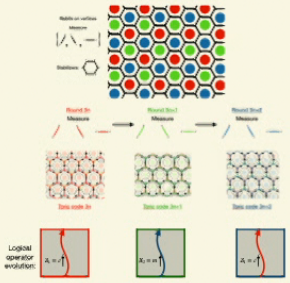

- Schedule special: measuring $XX \to YY \to ZZ \to XX \to \dots$ does not produce above features.

Qudit generalization

- Generalizable to $\mathbb{Z}_N$ qudits:
  - ★ $\dots \to \mathbb{Z}_N$ TC $\to \mathbb{Z}_N$ TC $\to \mathbb{Z}_N$ TC $\to \mathbb{Z}_N$ TC $\to \dots$
  - ★ $e \to m$ automorphism after on full cycle of the schedule
  - ★ Can introduce em defect line
- Can be used to prepare any abelian twisted quantum double

Eg. $\mathbb{Z}_4$ toric code $\xrightarrow{\text{condense } e^2/m^2}$ $\{1, em, em^3, e^2\}$ Double semion theory

- Defects in qudit case can by manipulated to implement full Clifford group

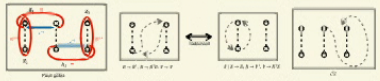

Adding a twist

- Adding twist defects in toric code introduces more logical qubits

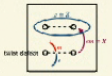

- We can implement these in the instantaneous toric codes which appear after each round of the Floquet code.
- To do this we modify schedule with two body operators corresponding to short em strings.
- Given large system we can create arbitrary many logical qubits by performing two body measurements

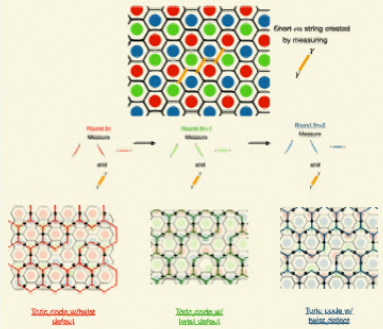

Acknowledgements and References

- Matthew B. Hastings and Jeongwan Haah, "Dynamically generated logical qubits," Quantum 5, 564 (2021).
- Alexei Kitaev, "Anyons in an exactly solved model and beyond," Annals of Physics 321, 2-111 (2006).
- Tyler D. Ellison, Yu-An Chen, Arpit Dua, Wilbur Shirley, Nathanan Tantivasadakarn, and Dominic J. Williamson, "Pauli stabilizer models of twisted quantum doubles," PRX Quantum 3, 010353 (2022).
- H. Bombin, "Topological order with a twist: Ising anyons from an abelian model," Phys. Rev. Lett. 105, 030403 (2010).
- Maissam Barkeshli, Hong-Chen Jiang, Ronny Thomale, and Xiao-Liang Qi, "Generalized Kitaev models and extrinsic non-abelian twist defects," Physical Review Letters 114 (2015).

3. Department of Physics, Yale University, New Haven, CT 06511, USA
4. Stewart Blusson Quantum Matter Institute, University of British Columbia, Vancouver, BC, Canada V6T 1Z1
5. Walter Burke Institute for Theoretical Physics, California Institute of Technology, Pasadena, CA 91125, USA
6. Department of Physics, Harvard University, Cambridge, MA 02138, USA

Background on Floquet codes

- Error correcting code inspired by the Kitaev honeycomb model
- Measurement schedule has three steps, involving measurement of two-body operators. After each round, half the qubits form a toric code eigenstate.
- Toric code is "moved around" in Hilbert space but logical information is preserved: dynamical logical qubit.
- Schedule constantly updates stabilzer eigenvalues allowing for error correction

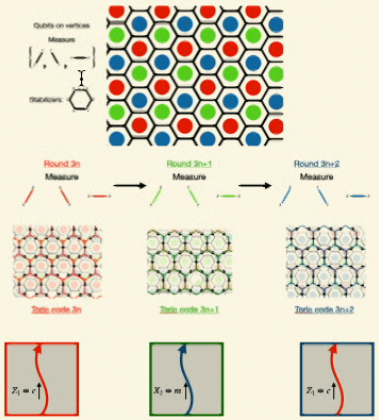

- Schedule special: measuring $XX \to YY \to ZZ \to XX \to \dots$ does not produce above features.

Qudit generalization

- Generalizable to $\mathbb{Z}_N$ qudits:
  - ★ $\dots \to \mathbb{Z}_N$ TC $\to \mathbb{Z}_N$ TC $\to \mathbb{Z}_N$ TC $\to \mathbb{Z}_N$ TC $\to \dots$
  - ★ $e \to m$ automorphism after on full cycle of the schedule
  - ★ Can introduce em defect line
- Can be used to prepare any abelian twisted quantum double

condense e^2m^2

Adding a twist

- Adding twist defects in toric code introduces more logical qubits

- We can implement these in the instaneous toric codes which appear after each round of the Floquet code.
- To do this we modify schedule with two body operators corresponding to short em strings.
- Given large system we can create arbitrary many logical qubits by performing two body measurements

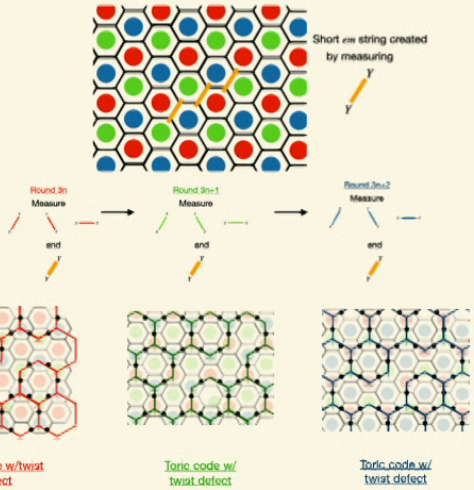

Acknowledgements

Overparameterization of Realistic Quantum Systems

Matthew Duschenes*, Juan Carrasquilla, Raymond Laflamme
University of Waterloo, Institute for Quantum Computing, & Vector Institute

November 14, 2022

PI Quantum Matter Workshop 2022

Learning Optimal Quantum Systems

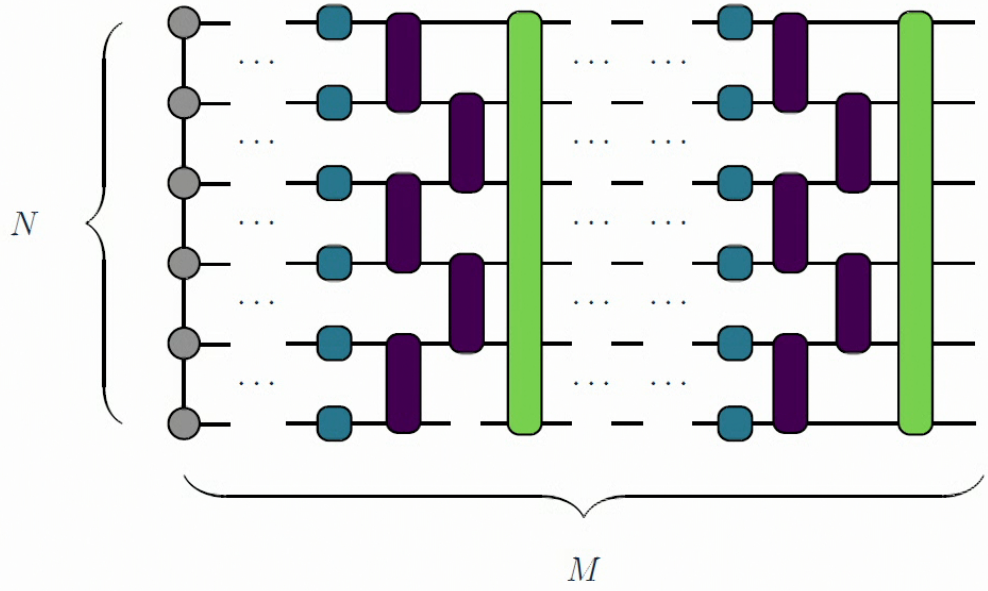

How does the amount of *noise* γ and the *evolution time* M
of a *constrained* system $\Lambda_{\theta\gamma}$
affect its optimization and resulting parameters θ?

VECTOR INSTITUTE

Constrained vs. Noisy Optimization

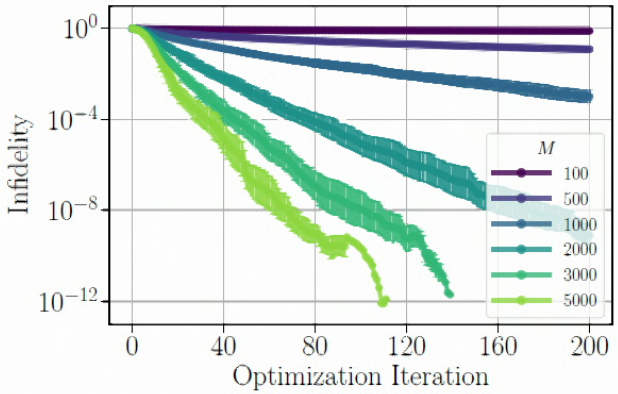

(a) Exponential Convergence of Constrained Infidelity

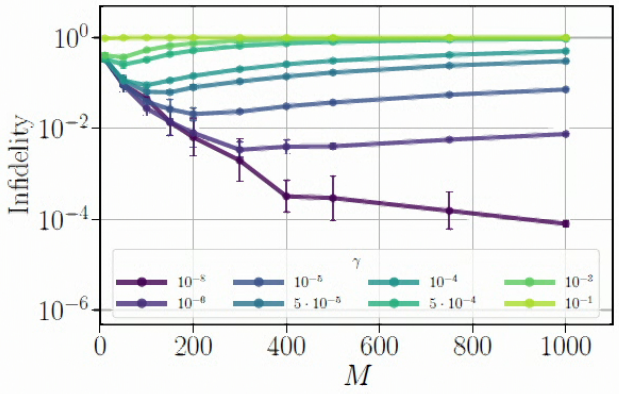

(b) Critical Depth for Noisy Infidelity

VECTOR INSTITUTE

Ultra-fast Entanglement Dynamics in Monitored Quantum Circuits

Shengqi Sang[1,2], Zhi Li[1], Timothy H. Hsieh[1], Beni Yoshida[1]
[1] Perimeter Institute for Theoretical Physics, Waterloo, Ontario N2L 2Y5, Canada
[2] Department of Physics and Astronomy, University of Waterloo, Waterloo, Ontario N2L 3G1, Canada

Monitored quantum circuit (MQC):

- Unitary operation: 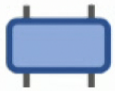
- Projective measurement: 

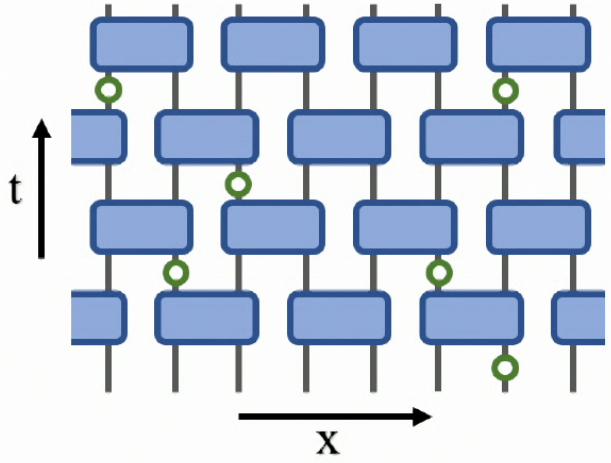

What we find in MQC…

- Entanglement generation:

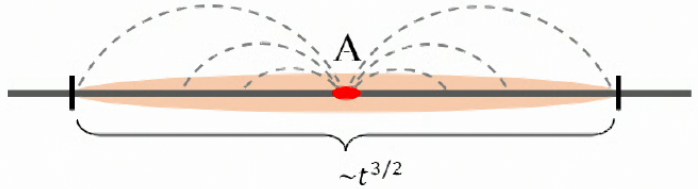

- Spreading of local information:

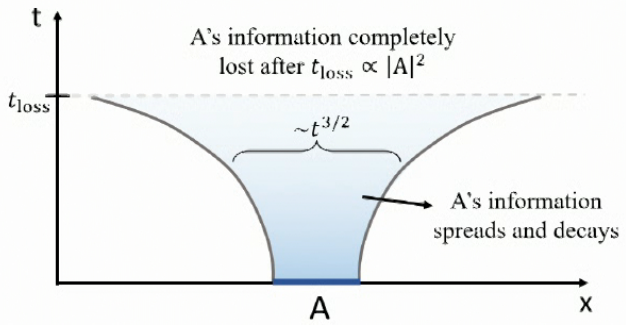

UV/IR Mixing in Marginal Fermi Liquid


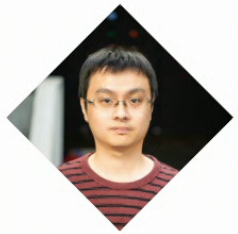

Weicheng Ye

Based on [arXiv: 2109.00004] with *Sung-Sik Lee, Liujun Zou*

- **Non-Fermi liquids(nFLs)/Marginal Fermi Liquids(MFL)** is central to the understanding of **superconductivity** as well as **strange metal**
- **UV/IR Mixing: Infrared** (IR) physics is sensitive to the *details* of the **Ultraviolet** (UV) description of the theory
- UV/IR mixing exists in the patch theory description of MFL

$$\Pi(k_\tau = 0, k_y) \sim \left(\ln\left(\frac{\Lambda_y}{k_y}\right)\right)^2$$

- To capture the low-energy physics of the whole Fermi surface, a natural theoretical framework is potentially the **functional renormalization group method**

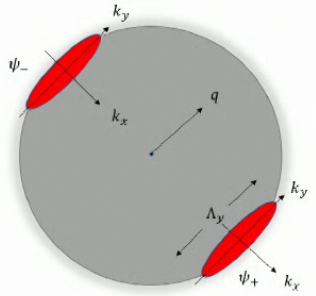

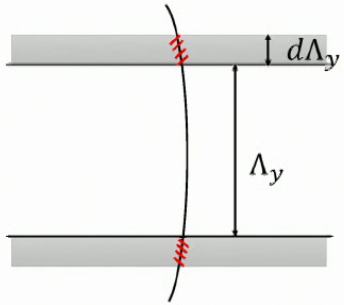

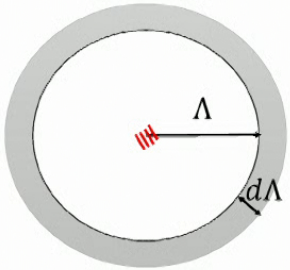

Quantum Physics in Highly Connected Worlds

A top-down graph-theoretic approach to the many-body problem

Joseph Tindall[1], Amy Searle[2], Abdulla Alhajri[2] and Dieter Jaksch[2]

[1]Center for Computational Quantum Physics, Flatiron Institute, New York
[2]Department of Physics, University of Oxford, United Kingdom

FLATIRON INSTITUTE
Center for Computational Quantum Physics

$$\mathcal{G} = \mathcal{G}(V, E)$$

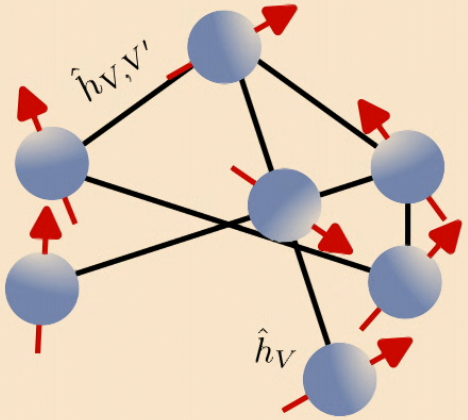

$$\hat{H}(\mathcal{G}) = \frac{L}{N_E}\left(\sum_{(v,v')\in E} \hat{h}_{v,v'}\right) + \sum_{v\in V} \hat{h}_v,$$

Free Energy Density:

$$f(\mathcal{G}) = -\tfrac{1}{L\beta}\ln\left(\mathrm{Tr}\left(\exp(-\beta H(\mathcal{G}))\right)\right)$$

J. Tindall et al, Quantum Physics in Connected Worlds, arXiv:2205.07924 (to appear in Nature Communications)

Quantum Physics in Highly Connected Worlds

A top-down graph-theoretic approach to the many-body problem

Joseph Tindall[1], Amy Searle[2], Abdulla Alhajri[2] and Dieter Jaksch[2]

[1]Center for Computational Quantum Physics, Flatiron Institute, New York
[2]Department of Physics, University of Oxford, United Kingdom

FLATIRON INSTITUTE
Center for Computational Quantum Physics

Theorem 1 *Let $G(L)$ be a graph drawn uniformly from the space of all simple, unweighted graphs over L vertices. Let $G_{\text{Complete}}(L)$ be the simple, unweighted graph over L vertices where all edges are present. Then we have*

$$\lim_{L\to\infty} f(G(L)) = \lim_{L\to\infty} f(G_{\text{Complete}}(L))$$

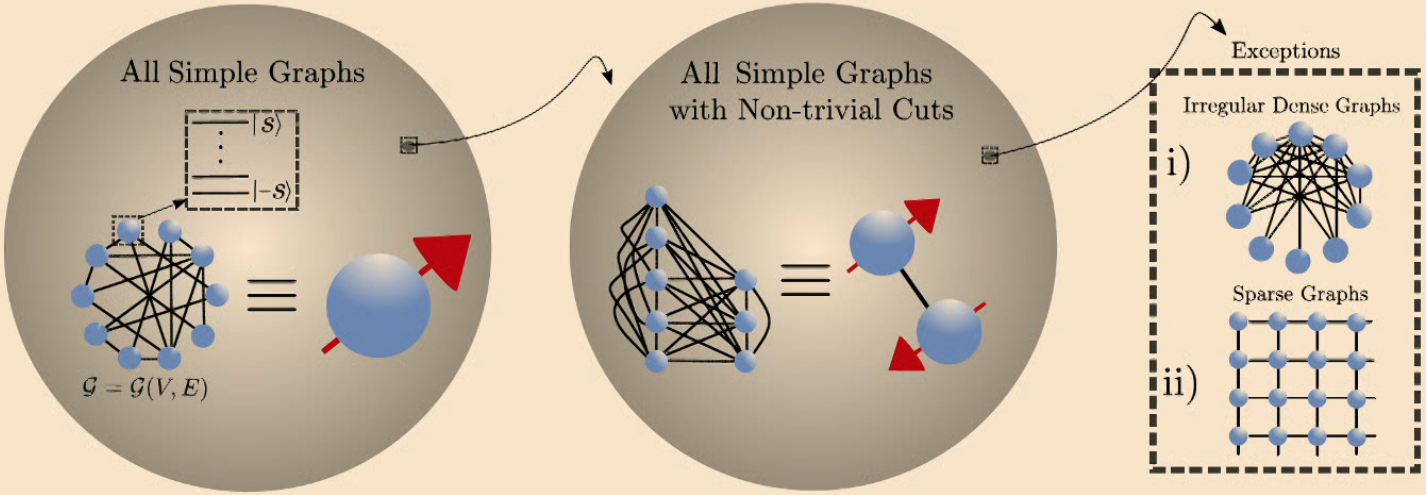

J. Tindall et al, Quantum Physics in Connected Worlds, arXiv:2205.07924 (to appear in Nature Communications)

Quantum Physics in Highly Connected Worlds

A top-down graph-theoretic approach to the many-body problem

Joseph Tindall[1], Amy Searle[2], Abdulla Alhajri[2] and Dieter Jaksch[2]

[1]Center for Computational Quantum Physics, Flatiron Institute, New York
[2]Department of Physics, University of Oxford, United Kingdom

FLATIRON INSTITUTE
Center for Computational Quantum Physics

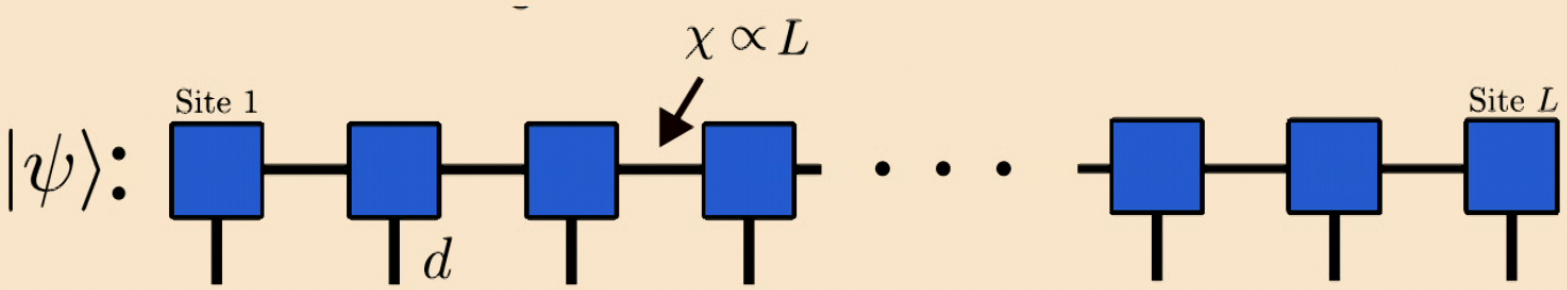

J. Tindall et al, Quantum Physics in Connected Worlds, arXiv:2205.07924 (to appear in Nature Communications)